

## Higher-order corrections to particle diffusion in strongly magnetized two-component plasmas

C. Deutsch

*Laboratoire de Physique des Plasmas, Bâtiment 212, Université Paris XI, 91405 Orsay Cédex, France*

(Received 30 September 1977)

The nodal expansion of equilibrium properties of a two-component classical plasma in  $2 + \epsilon$  dimensions ( $0 \leq \epsilon \leq 1$ ) is used to investigate higher-order corrections with respect to the plasma parameter of the transverse-diffusion coefficient relative to an arbitrarily strong and constant magnetic field. Only the short-range compact nodal graphs decaying faster than Debye contribute to the third and higher nonvanishing orders. The usual fluid-limit ( $k \rightarrow 0$ ) procedure delivering the first-order Bohm result is shown to be self-consistent for any dimension  $2 \leq \nu \leq 3$ .

### I. INTRODUCTION

The diffusion of plasma transverse to an arbitrarily strong constant magnetic field is a subject of basic importance in classical plasma physics. It has direct relevance to the confinement of ionized gases sufficiently hot to sustain exo-energetic nuclear reactions yielding thermal neutrons.<sup>1,2</sup> Up to now, attention has been focused on the stochastic assumptions underlying the many different, although nearly equivalent, derivations of the Bohm transverse diffusion coefficient  $D_{\perp} \sim B^{-1}$  in two and three dimensions. These assumptions are in agreement with general scaling arguments.<sup>3</sup> All these treatments, without exception, make use of a fluid picture of the two-component plasma (hereafter referred to as TCP). The screening length  $\lambda_D$  is assumed to be very large, while the dynamics is taken as a function of first-order equilibrium properties with respect to the plasma parameter. Here we shall not enter into the details of more sophisticated calculations<sup>3</sup> based on the microscopic Klimontovitch time-dependent one- and two-particle distribution functions, which yield essentially the same results. Our main purpose is the systematic investigation of high-order corrections in the plasma parameter  $\Lambda$  to  $D_{\perp}^2$ , irrespective of the space dimension  $2 \leq \nu \leq 3$ . Therefore the more traditional approach used in Refs. 1 and 2 will prove sufficient for our present needs. In this case, the TCP's equilibrium properties are simply obtained by duplicating those of the standard one-component plasma (OCP in the sequel) model. As shown below, such an approximation is valid only when one's attention is restricted to the first-order Debye term.

A recent detailed investigation<sup>4</sup> of the TCP pair correlation function has shown that the neutrality condition prevents the extension of the previous treatments<sup>1,2</sup> based upon the above assumption, to all order in  $\Lambda$ . The importance of the higher corrections to  $D_{\perp}^2$  is motivated by several distinct con-

siderations. First, there is the need of a deeper understanding of the fluid picture underlying all the derivations of the Bohm result. In other words, even in a very hot and dilute plasma with a very large  $\lambda_D$ , we should check that higher-order terms are consistently negligible when compared to the first terms so that we can allow for a coherent use of the perturbation expansion in  $\Lambda$ . Of more direct relevance to experimental fusion research, we should also mention that the present most successful Tokamak device<sup>5</sup> works at a relatively moderate temperature, i.e.,  $T \sim 1$  keV instead of the expected 10 keV. However, the basic need for the present investigation arises from the pathological, although probable, situations occurring in laser fusion<sup>6</sup> when huge, self-generated magnetic fields (up to  $10^6$  G) produce hot spots and very severely inhibit the heat penetration from the underdense outside high-temperature plasma toward the dense core of the pellet.

Last, but not least, the strongly magnetized TCP allows for a clear and relatively simple investigation of transport quantities independent of time. Such a fortunate situation is due to the drastic modeling of the particle dynamics within the framework of the guiding center approximation valid for this case. We should also notice that our continuous parametrization of the equilibrium nodal expansion with respect to the space dimensionality  $\nu = 2 + \epsilon$  gives access to an elegant unified presentation of the hydrodynamic calculation of the Bohm velocity diffusion coefficient.

### II. BASIC THEORY

In this work we address ourselves to the evaluation of the time-independent transverse diffusion coefficient to a very large constant magnetic field  $B$ , in a high-temperature fully ionized TCP. The mean kinetic energy per particle is assumed to be high enough to allow the neglect of any symmetry (Fermi) contribution to the equilibrium properties.

The only retained  $\hbar \neq 0$  effect is due to the uncertainty principle through the inequality  $\hbar/\sqrt{2m_{ei}k_B T} > e^2/k_B T$  which means  $k_B T > 1$  Ry in three dimensions.<sup>13</sup> These nonzero diffraction corrections usually unnoticed in high-temperature fusion physics are non-negligible only for small distances comparable to the Bohr radius  $a_0$ . So, the hydrodynamic modes (convective cells, for instance) supposed to convey most of the particle transport across  $\vec{B}$  are not affected by them. Moreover, we shall work with the very plausible assumption that  $\vec{B}$  does not change the TCP equilibrium properties. In other words, the Bohr-Van Leuween theorem applies to the electron wave packets which we assume, for simplicity, to be spinless. With this proviso in mind, we may reformulate the three-dimensional derivation detailed in Refs. 2 in a framework varying with the dimension.

With the exception of the  $\nu$  unification and the ensuing fractal geometry of the transverse diffusion, the present section is essentially a review of the hydrodynamic derivation detailed in Refs. 2. We will take our concept of a real dimension  $\nu = 2 + \epsilon$  as the simpler<sup>7</sup> to secure a smooth transition between  $\nu = 2$  and 3. In so doing, we shall use Wilson techniques<sup>8</sup> for the interpolation of quadratures and the redefinition of vectors in Euclidian (not vectorial!) spaces with noninteger  $\nu$  value. Therefore, the transverse velocity coefficient extending the  $\nu = 2$  model of charged filaments<sup>1,2</sup> aligned with  $\vec{B}$  obtains as ( $c$  being the speed of light)

$$D_{\perp} = \frac{c^2}{B^2} \int_0^{\infty} \langle \vec{E}_{\perp}(0) \cdot \vec{E}_{\perp}(\tau) \rangle d\tau \quad (2.1)$$

in terms of the autocorrelation function of the electric field  $\vec{E}(\tau)$  seen by a test charge a time  $\tau$ , with the guiding center approximation

$$\vec{X}(t) = c \int_0^t \frac{\vec{E}(\tau) \times \vec{B}}{B^2} d\tau. \quad (2.2)$$

The bracket denotes the usual canonical equilibrium average. To go farther we need a redefinition of the point and cross vector products. This is easily achieved by taking the same scalar product while the vectorial one is interpolated by an infinite matrix arising from the infinite number of vector components in a Euclidian space with real  $\nu$ .<sup>8</sup> Only for  $\nu$  integer the number of mutual perpendiculars at a given point could be identified with the space dimension. The corresponding integrals should read

$$\int d^{\nu} \vec{p} f(p^2, \vec{p} \cdot \vec{a}_1, \vec{p} \cdot \vec{a}_2, \dots) (2\pi)^{-\nu}.$$

Moreover, we take for granted the existence of the discrete sum

$$\vec{E}(\tau) = \sum_{\vec{k}} \vec{E}_{\vec{k}}(\tau) e^{i\vec{k} \cdot \vec{X}(\tau)}$$

for all  $2 \leq \nu \leq 3$ . The problem is one of evaluating the electric field auto-correlation  $\langle \vec{E}_{\perp}(0) \cdot \vec{E}_{\perp}(\tau) \rangle$  when  $\vec{E}(\tau)$  is the electric field seen at time  $\tau$  by a "test ion" located on the  $z$  axis at  $\tau = 0$ .  $\vec{E}(\tau)$  is related to the Eulerian electric field  $\vec{E}(\vec{X}, t)$  by  $\vec{E}(\tau) = \vec{E}[\vec{X}(\tau), \tau]$  and

$$\begin{aligned} \vec{E}(\vec{X}, t) &= \sum_{\vec{k}} \sum_j \frac{4\pi\vec{k}}{ik^2} \frac{e_j}{V} e^{i\vec{k} \cdot [\vec{X} - \vec{X}_j(t)]} \\ &= \sum_{\vec{k}} \vec{E}_{\vec{k}}(t) e^{i\vec{k} \cdot \vec{X}}. \end{aligned} \quad (2.3)$$

The present Fourier expansion holds for all  $0 \leq \epsilon \leq 1$ , because

$$\vec{E}_{\vec{k}}(t) = \int d^{\nu} \vec{x} e^{-i\vec{k} \cdot \vec{x}} \vec{E}(\vec{x}, t)$$

is meaningful for any  $k$ .  $\vec{X}(\tau)$  is the orbit of the test particle, while  $\vec{X}_j(t)$  is the location of the  $j$ th charge at time  $t$ . In Eq. (2.2) the bracket is explained so that

$$D_{\perp} = \frac{c^2}{B^2} \int_0^{\infty} \sum_{\vec{k}} \langle \vec{E}_{\perp\vec{k}}^*(0) \cdot \vec{E}_{\perp\vec{k}}(\tau) e^{i\vec{k} \cdot \vec{X}(\tau)} \rangle d\tau. \quad (2.4)$$

Furthermore, we will ignore the correlation between the position of the test particle and those of the background plasma [the  $\vec{X}(\tau)$ ]. This amounts to saying that  $|g_2^{ij}(\nu) - 1| < 1$  [ $g_2^{ij}(\nu)$  denotes any one of the three TCP pair correlation functions], even when higher-order corrections are retained. Such an assumption restricts us to plasma parameter values smaller than unity. Since  $\langle \vec{E}_{\vec{k}_1} \cdot \vec{E}_{\vec{k}_2} \rangle = 0$  for  $\vec{k}_1 \neq -\vec{k}_2$  and a spatially uniform ensemble, we have the statistical factorized result

$$D_{\perp} = \frac{c^2}{B^2} \int_0^{\infty} \sum_{\vec{k}} \langle \vec{E}_{\perp\vec{k}}^*(0) \cdot \vec{E}_{\perp\vec{k}}(\tau) \rangle \langle e^{i\vec{k} \cdot \vec{X}(\tau)} \rangle d\tau \quad (2.5)$$

evaluated when  $\exp[i\vec{k} \cdot \vec{X}(\tau)]$  is known, while the first average reads

$$\begin{aligned} \langle \vec{E}_{\perp\vec{k}}^*(0) \cdot \vec{E}_{\perp\vec{k}}(\tau) \rangle &= \sum_{i,j} \frac{S_{\nu}^2 e_i e_j}{k^2 V^2} \frac{k_1^2}{k^2} \\ &\quad \times \langle \exp^{i\vec{k} \cdot [\vec{X}_i(\tau) - \vec{X}_j(0)]} \rangle, \end{aligned} \quad (2.6)$$

where  $S_{\nu} = 2\pi^{\nu/2}/\Gamma(\frac{1}{2}\nu)$ . Extending in a straightforward way the  $\nu = 2$  and 3 trajectories, we have

$$\begin{aligned} \vec{X}(\tau) &= \vec{X}(0) + c \int_0^{\tau} \frac{\vec{E}(\tau') \times \vec{B}}{B^2} d\tau' + \hat{b} V_{\parallel} t \\ &\quad + \int_0^{\tau} d\tau' \int_0^{\tau'} d\tau'' e_i \frac{\hat{b} \cdot \vec{E}(\tau'') \hat{b}}{m_i}. \end{aligned} \quad (2.7)$$

$\hat{b}$  is the unit vector  $\parallel \vec{B}$ . The test charge is taken to be an ion with charge-to-mass ratio  $e_i/m_i$ . The initial position  $\vec{X}(0)$  may be set equal to zero, while the initial test ion velocity  $V_{\parallel}$  is a statistically distributed quantity assumed to obey the Boltzmann distribution. Evaluating  $\langle \exp[i\vec{k} \cdot \vec{X}(\tau)] \rangle$  is no simple matter. About the best that can be done is the following. Because  $\vec{X}(\tau)$  is the portion of a random variable initially localized near  $\vec{X}(0)=0$ , and because its probability distribution  $P[\vec{X}(\tau), \tau]$  is expected to spread out with time,

$$\langle \exp[i\vec{k} \cdot \vec{X}(\tau)] \rangle = \int d\vec{X}(\tau) e^{i\vec{k} \cdot \vec{X}(\tau)} P[\vec{X}(\tau), \tau]$$

will damp with increasing  $\tau$  for any  $\epsilon > 0$ . The damping occurs for two reasons: motions "parallel" and "perpendicular" to  $\vec{B}$ . Only the latter is operative when  $\epsilon = 0$ . The damping along  $B$  will be more extreme than that due to the "perpendicular" motion. Therefore, in the presence of very strong magnetic fields, it is useful to forget the "perpendicular" drift except when  $\vec{k} \perp \vec{B}$ . This is tantamount to assuming

$$\langle e^{i\vec{k} \cdot \vec{X}(\tau)} \rangle = \begin{cases} \left\langle \exp\left(\frac{ic\vec{k} \times \vec{B}}{B^2} \int_0^\tau \vec{E}(\tau') d\tau'\right) \right\rangle, & \vec{k} \cdot \vec{B} = 0 \\ \left\langle \exp\left[ic\vec{k} \cdot \left(\hat{b}V_{\parallel}\tau + \int_0^\tau d\tau' \int_0^{\tau'} d\tau'' e_i \hat{b} \cdot \frac{\vec{E}(\tau'')}{m_i}\right)\right] \right\rangle, & \vec{k} \cdot \vec{B} \neq 0. \end{cases} \quad (2.8)$$

The "parallel" electric field can accelerate a particle for any  $\epsilon > 0$ , whereas the "perpendicular" component cannot.

The "perpendicular" motion can be visualized as a limit of small increments in position space, the "parallel" motion as a sum of small increments in velocity space. This picture is the  $\nu=3$  one extended to any  $\nu > 2$ . Eventually some of the particles will move rapidly. They will begin to lose energy through the radiation of plasma oscillations, and the relatively infrequent close collisions with other particles. So, the electric field seen in the "parallel" direction is not well modeled by a velocity-independent distribution probability. The "parallel" motion is closer to the Langevin approximation of the linear Brownian motion. It should be appreciated that a Brownian motion<sup>9</sup> may be given any dimension in the framework of the so-called fractal geometry. Therefore, the required interpolation between  $\nu=2$  and 3 could easily be supplied by motions with dimensions smaller than one, provided a fractal dimension exists for any  $\nu$ , defined in the present Wilson meaning. We take this plausible point for granted,<sup>10</sup> so a given test particle will obey

$$\frac{dV}{dt} = -F(V) + A(t) \quad (2.9)$$

with a frictional drag coefficient  $F(V)$  and a stationary random force field  $A \approx \hat{b}\hat{b} \cdot \vec{E}(t)$ . In this approach the dimensions of the ensemble spanned in the "parallel" motion should be derived from  $F(V)$

and  $A(t)$ . Devoting our main effort to the higher-order corrections in the plasma parameter we do not need to explore this subject more quantitatively. At this point, we need an approximation which will render tractable the second expression in the right-hand side of Eq. (2.8). One possible procedure is to neglect the contribution of the "parallel" electric field. So, we extrapolate the  $\nu=2$  case and therefore concentrate on the low-frequency long-wavelength parts of the electric field spectrum. For this reason, one may expect the mechanism of free streaming of particles down the field lines to be dominant in destroying the correlations between the initial electric field seen by a particle and that field at a later time. If we ignore  $E_{\parallel}$ , we get for  $\vec{k} \cdot \vec{B} \neq 0$ ,

$$\langle e^{i\vec{k} \cdot \vec{X}(\tau)} \rangle_{k_{\parallel} \neq 0} \equiv \langle \exp(ic\vec{k} \cdot \hat{b}V_{\parallel}\tau) \rangle = \exp\left(-\frac{1}{2}k_{\parallel}^2 V_{\text{ion}}^2 \tau^2\right),$$

where we have assumed the test ions to be distributed with a thermal equilibrium velocity  $V_{\text{ion}}^2 \equiv k_B T/m_i$ . Generalizing the  $\nu=2$  treatment<sup>2</sup> thus gives

$$\langle \exp[i\vec{k} \cdot \vec{X}(\tau)] \rangle_{k_{\parallel}=0} = \exp\left(-\frac{c^2 k^2}{4B^2} \int_0^\tau d\tau_1 \int_0^{\tau_1} d\tau_2 \langle \vec{E}_{\perp}(\tau_1) \cdot \vec{E}_{\perp}(\tau_2) \rangle\right) \quad (2.10)$$

for the case of purely perpendicular  $\vec{k}$ 's. Also, making the approximation that led to Eq. (2.10) we see

$$\begin{aligned}
\langle \vec{E}_{i\vec{k}}^*(0) \cdot \vec{E}_{i\vec{k}}(\tau) \rangle &= \sum_{i,j} \frac{S_v^2 e_i e_j}{k^2 V^2} \frac{k_1^2}{k^2} \langle \exp i\vec{k} \cdot [\vec{X}_i(0) - \vec{X}_j(0)] \rangle \exp(-\frac{1}{2} k_{\parallel}^2 V_{0j}^2 \tau^2), \quad k_{\parallel} \neq 0 \\
&= \sum_{i,j} \frac{S_v^2 e_i e_j}{k_1^2 V^2} \exp\left(-\frac{c^2 k^2}{4B^2} \int_0^{\tau} d\tau_1 \int_0^{\tau} d\tau_2 \langle \vec{E}_1(\tau_1) \cdot \vec{E}_1(\tau_2) \rangle\right) \langle \exp i\vec{k} \cdot [\vec{X}_i(0) - \vec{X}_j(0)] \rangle, \quad k_{\parallel} = 0
\end{aligned} \quad (2.11)$$

where  $V_{0j}^2 \equiv k_B T / m_j$ . Finally, we need

$$\langle \exp i\vec{k} \cdot [\vec{X}_i(0) - \vec{X}_j(0)] \rangle = \delta(\vec{k}) - \frac{\int d^v \vec{r} g_2^{ij}(r) e^{-i\vec{k} \cdot \vec{r}}}{V} \equiv \delta(k) - V^{-1} S_{ij}(k). \quad (2.12)$$

Inserting Eqs. (2.11) and (2.12) into

$$\langle \vec{E}_1(0) \cdot \vec{E}_1(\tau) \rangle = \sum_{\vec{k}} \langle \vec{E}_{i\vec{k}}(0) \cdot \vec{E}_{i\vec{k}}(\tau) \rangle \langle e^{i\vec{k} \cdot \vec{x}(\tau)} \rangle \quad (2.13)$$

we have

$$\begin{aligned}
\langle \vec{E}_1(0) \cdot \vec{E}_1(\tau) \rangle &= \sum_{i=j} \sum_{\substack{\vec{k} \\ k_{\parallel} \neq 0}} \frac{S_v^2 e_i e_j}{k^2 V^2} \frac{k_1^2}{k^2} \exp\left(-\frac{k_{\parallel}^2 V_{0j}^2 \tau^2}{2}\right) \exp\left(-\frac{k_{\parallel}^2 V_{10n}^2 \tau^2}{2}\right) \\
&+ \sum_{i=j} \sum_{\substack{\vec{k} \\ k_{\parallel} = 0}} \frac{S_v^2 e_i e_j}{k^2 V^2} \exp\left(-\frac{c^2 k_1^2}{2B^2} \int_0^{\tau} d\tau_1 \int_0^{\tau} d\tau_2 \langle \vec{E}_1(\tau_1) \cdot \vec{E}_1(\tau_2) \rangle\right) \\
&+ \sum_{i \neq j} \sum_{\substack{\vec{k} \\ k_{\parallel} \neq 0}} \frac{S_v^2 e_i e_j}{k^2 V^2} \frac{k_1^2}{k^2} \exp\left(-\frac{k_{\parallel}^2 V_{0j}^2 \tau^2}{2}\right) [\delta(k) - S_{ij}(k) V^{-1}] \exp(-\frac{1}{2} k_{\parallel}^2 V_{10n}^2 \tau^2) \\
&+ \sum_{i \neq j} \sum_{\substack{\vec{k} \\ k_{\parallel} = 0}} \frac{S_v^2 e_i e_j}{k^2 V^2} \exp\left(-\frac{c^2 k_1^2}{2B^2} \int_0^{\tau} d\tau_1 \int_0^{\tau} d\tau_2 \langle \vec{E}_1(\tau_1) \cdot \vec{E}_1(\tau_2) \rangle\right) [\delta(k) - S_{ij}(k) V^{-1}], \dots
\end{aligned} \quad (2.14)$$

This is an integral Eq. for  $\langle \vec{E}_1(0) \cdot \vec{E}_1(\tau) \rangle$ . Performing the  $i, j$  summation makes the  $\delta(k)$  contribution cancel out altogether with the first two sums thus yielding

$$\begin{aligned}
\langle \vec{E}_1(0) \cdot \vec{E}_1(\tau) \rangle &= \sum_{\substack{\vec{k} \\ k_{\parallel} \neq 0}} \frac{S_v^2 e^2 k_1^2}{k^4 V^2} \exp\left(-\frac{k_{\parallel}^2 V_{0j}^2 \tau^2}{2}\right) \exp\left(-\frac{k_{\parallel}^2 V_{10n}^2 \tau^2}{2}\right) \mathcal{C}(k) \\
&+ \sum_{\substack{\vec{k} \\ k_{\parallel} = 0}} \frac{S_v^2 e^2}{k^2 V^2} \exp\left(-\frac{c^2 k_1^2}{2B^2} \int_0^{\tau} d\tau_1 \int_0^{\tau} d\tau_2 \langle \vec{E}_1(\tau_1) \cdot \vec{E}_1(\tau_2) \rangle\right) \mathcal{C}(k),
\end{aligned} \quad (2.15)$$

where

$$\mathcal{C}(k) = V^{-1} (-S_{ee}(k) - S_{ii}(k) + 2S_{ei}(k)) \quad (2.16)$$

is the extension of the usual first-order thermal spectrum. Equation (2.15) can be simplified through

$$\frac{1}{2} \langle \vec{E}_1(0) \cdot \vec{E}_1(\tau) \rangle \equiv Q_1(\tau),$$

$$R_1(\tau) \equiv \frac{c^2}{2B^2} \int_0^{\tau} d\tau_1 \int_0^{\tau} d\tau_2 Q_1(\tau_2 - \tau_1),$$

$$\frac{d^2 R_1(\tau)}{d\tau^2} = \frac{c^2 Q_1(\tau)}{B^2}$$

in the form

$$\begin{aligned}
2Q_1(\tau) &= \frac{S_v^2 e^2}{V^2} \sum_{\substack{\vec{k} \\ k_{\parallel} \neq 0}} \frac{k_1^2}{k^2} \mathcal{C}(k) \exp(-\frac{1}{2} k_{\parallel}^2 V_{10n}^2 \tau^2) \\
&\quad \times \exp(-\frac{1}{2} k_{\parallel}^2 V_{0j}^2 \tau^2) \\
&+ \sum_{\substack{\vec{k} \\ k_{\parallel} = 0}} \frac{S_v e^2}{k^2 V^2} \exp[-2k_1^2 R_1(\tau)] \mathcal{C}(k),
\end{aligned} \quad (2.16')$$

Defining  $\epsilon_b = S_v^2 e^2 c^2 / B^2 V^2 k_D^2$ , this becomes, replacing  $\tau$  by  $t$

$$\frac{d^2 R_{\perp}(\tau)}{d\tau^2} = \epsilon_b \sum_{\substack{\vec{k} \\ k_{\parallel} \neq 0}} \exp[-2k_{\perp}^2 R_{\perp}(\tau)] \mathcal{C}(k) k^2 + \epsilon_b \sum_{\substack{\vec{k} \\ k_{\parallel} \neq 0}} f(\vec{k}, t) \quad (2.17)$$

which can be integrated, when one notes that  $dR_{\perp}(0)/dt = 0$ , in the form

$$\frac{dR_{\perp}(t)}{dt} = \epsilon_b \sum_{\substack{\vec{k} \\ k_{\parallel} \neq 0}} \int_0^t d\tau e^{-2k_{\perp}^2 R_{\perp}(\tau)} \mathcal{C}(k) + \epsilon_b \sum_{\substack{\vec{k} \\ k_{\parallel} \neq 0}} \int_0^t f(\vec{k}, \tau) d\tau \quad (2.18)$$

The only place the magnetic field enters the above equations is in the denominator of the small quantity  $\epsilon_b$ . Therefore, we seek the leading term, in powers of  $\epsilon_b$ , of the solutions to Eqs. (2.17) and (2.18). We shall see presently that for large  $t$ ,  $R(t) \sim \epsilon_b^{1/2} t$  makes the first term on the right-hand side of Eq. (2.18) an  $O(\epsilon_b^{1/2})$  term. Since the second is  $O(\epsilon_b)$ , it can be deleted to the lowest significant orders in  $\epsilon_b$ , either in (2.18) or in (2.17). If we delete  $f(\vec{k}, t)$  in Eq. (2.17), we get ( $k^2 = k_{\perp}^2 + k_{\parallel}^2$ )

$$\frac{d^2 R_{\perp}(t)}{dt^2} \cong \epsilon_b \sum_{\substack{\vec{k} \\ k_{\parallel} \neq 0}} e^{-2k_{\perp}^2 R_{\perp}(t)} \mathcal{C}(k) \quad (2.19)$$

or equivalently

$$\frac{1}{2} \left( \frac{dR_{\perp}(t)}{dt} \right)^2 = \frac{\epsilon_b}{2} \sum_{\vec{k}_{\perp}} \left( \frac{1 - \exp(-2k_{\perp}^2 R_{\perp})}{k_{\perp}^2} \right) \mathcal{C}(k). \quad (2.20)$$

Since  $R_{\perp}$  and its first two derivatives are always positive for  $t > 0$ , the last term in Eq. (2.20) becomes negligible at  $t \rightarrow \infty$ , and

$$\frac{1}{2} \left( \frac{dR_{\perp}(\infty)}{dt} \right)^2 = \frac{\epsilon_b}{2} \sum_{\vec{k}_{\perp}} \frac{\mathcal{C}(k)}{k_{\perp}^2}. \quad (2.21)$$

But  $\frac{1}{2} D_{\perp}$  is just  $dR_{\perp}(\infty)/dt$ , so

$$D_{\perp} = 2\epsilon_b^{1/2} \sum_{\vec{k}_{\perp}} \left( \frac{\mathcal{C}(k)}{k_{\perp}^2} \right)^{1/2} + O(\epsilon_b). \quad (2.22)$$

To approximate it by an integral for a large volume, we make the replacement<sup>8</sup>

$$\sum_{\vec{k}} \rightarrow \frac{V^{2/\nu}}{2\pi} \int_{k_{\min}}^{k_D} k_{\perp} dk_{\perp}. \quad (2.23)$$

$k_{\min} = 2\pi/V^{1/\nu}$  is the lower limit which results from the finite box size, while the upper  $k_D = \lambda_D^{-1}$  means that we restrict to the so-called fluid limit.<sup>1,2</sup>

### III. TWO-COMPONENT PLASMA EQUILIBRIUM PROPERTIES

Our task will be completed by explaining the structure factors sum (2.16) in terms of the higher-order corrections with respect to the plasma parameter. For this purpose, we need two things. The first is a smooth extension of the Coulomb interaction with respect to the dimensionality parameter  $\nu = 2 + \epsilon$ . This requirement is easily fulfilled by the potential

$$\begin{aligned} \phi^{(\nu)}(r) &= (\nu - 2)^{-1} |r|^{2-\nu}, \quad \nu \neq 2 \\ &= \ln |r|^{-1}, \quad \nu = 2. \end{aligned} \quad (3.1)$$

Solution of the Poisson equation is

$$\Delta \phi^{(\nu)}(r) = -|\nu - 2| S_{\nu} \delta_{\nu}(r). \quad (3.2)$$

The Fourier isometries between Eq. (3.1) and the Fourier transformation  $-S_{\nu} k^{-2}$  of Eq. (3.2) are obtained through the  $\nu$ -dependent Wilson quadratures<sup>9</sup> [ $K_{\nu} = S_{\nu} (2\pi)^{-\nu}$ ]

$$\begin{aligned} (2\pi)^{-\nu} \int d^{\nu} \vec{k} f(\vec{k} \cdot \vec{k}_1) \\ = \frac{K_{\nu-1}}{2\pi} \int_0^{\infty} dk \int_0^{\pi} d\phi k^{\nu-1} (\sin\phi)^{\nu-2} \\ \times f(k^2, k_1 k \cos\phi). \end{aligned} \quad (3.3)$$

The second equation requires the extension of the standard OCP nodal expansion<sup>7</sup> to the pointlike two-component plasmas with respect to the classical plasma parameter  $\Lambda_c = e^2/k_B T \lambda_D^{\epsilon}$  ( $\lambda_D^2 = k_B T / S_{\nu} \rho e^2$ ). The fulfillment of this latter condition is strongly  $\nu$  dependent. For  $\nu \leq 2$ , the corresponding classical  $2N$ -body systems are stable, so the TCP nodal expansion is obtained immediately from the OCP's by retaining the condition of neutrality. The situation is not so simple when  $\nu > 2$ . Here, Schrödinger quantum mechanics have to be retained to secure stability within the plus-minus pair, through the appearance of bound states down to a ground state with a negative finite energy. Nevertheless, a detailed study<sup>4</sup> shows that the perturbative expansion in  $\Lambda_c$  remains valid when  $k_B T$  is larger or comparable to the ground-state energy. This amounts to saying that the mean thermal energy should be high enough to break up almost any bound states. The degree of ionization is therefore very close to unity, which allows to work out the equilibrium properties in the canonical ensemble. However, there is an additional price to pay before employing quantum statistical mechanics so easily. To secure two-body stability in classical statistical mechanics, the long-range Coulomb interaction has to be interpolated with the  $r \rightarrow 0$  limit of the plus-minus Slater sum re-

stricted to the strongest interacting states in the continuum, i.e., the  $S$  states with  $l=0$ . In three dimensions this procedure leads to the replacement of  $r^{-1}$  by  $r^{-1}(1 - e^{-Cr})$  with  $C \sim \lambda_{ei}^{-1}$ .

An additional quantum-mechanical requirement is

$$\begin{aligned} \lambda_{ei} < \text{mean interparticle distance} < \lambda_D, \\ \Lambda_e \leq 1, \end{aligned} \tag{3.4}$$

still leaving room for substantial high-order improvements. With all these provisos in mind, we could perform the  $g_2^{ij}(r) - \Lambda_e$  expansion. Nevertheless, we should be cautious about the inclusion of a strong constant magnetic field in the above classical program. This point is discussed further in a separate work, where it is shown that in the realistic limit of a strong but still perturbative Zeeman interaction, the temperature-dependent pseudopotential built upon the spherical hydrogenic wave functions with  $B=0$ , remains unchanged in the present situation. The same is true of the electron-electron effective interaction including the  $\hbar \neq 0$  diffraction corrections.<sup>11</sup>

These preliminaries allow us to extend the  $\nu$ -dependent OCP  $\Lambda_e$  expansion<sup>7</sup> to the high-temperature pointlike TCP. So, the usual nodal rules are to be modified as follows.

(a) The screening length is such that

$$\lambda_D^2 = k_B T / S_\nu \rho e^2 (C_1 Z_1^2 + C_2 Z_2^2),$$

where  $C_i = N_i / NZ_i$  is the charge attached to the component  $i$ . Each field point gets an extra factor  $(C_1 Z_1^2 + C_2 Z_2^2)^{-1}$ .

(b) The interaction between particles  $i$  and  $j$  is proportional to  $Z_i Z_j$ , so that each field point is again factorized out with  $C_1 Z_1^{\Pi_k} + C_2 Z_2^{\Pi_k}$ , where  $\Pi_k$  denotes the number of lines merging into the field point  $k$ . The root points have to be given a factor  $Z_1^{\Pi_1} Z_2^{\Pi_2}$ .

(c) When  $\epsilon > 0$ , the Debye line  $k^2 + 1$ , which corresponds to the bare Coulomb interaction  $r^{-\epsilon}$ , has to be replaced by a normalized sum of the modified Debye lines attached to the direction ion-ion, ion-electron, electron-electron interactions, respectively. This is easily performed for  $\nu = 3$ , once we note that the Debye interaction resumming the long-range behavior of the effective interaction  $r^{-1}(1 - e^{-Cr})$  may be written  $(C\lambda_D > 2)$

$$\frac{e^2}{r} \frac{(e^{-\alpha_1 r} - e^{-\alpha_2 r})}{(1 - 4C^2/\lambda_D^2)^{1/2}}, \quad \frac{1}{k^2 + \alpha_1^2} - \frac{1}{k^2 + \alpha_2^2}, \tag{3.5}$$

in  $r$  and  $k$  space, respectively. Similar expressions may be worked out for the whole  $2 < \nu < 3$  range.

(d) Putting together the above rules for the field points, we see that each nodal graph with  $k$  field

points has to be given a factor  $(Z_1^{\Pi_{k-1}} - Z_2^{\Pi_{k-1}}) / (Z_1 - Z_2)$  when the overall neutrality condition  $C_1 Z_1 + C_2 Z_2 = 0$  is taken into account. As a consequence, the usual OCP linear chains built upon two bubbles intertwined with Debye lines vanish to all orders, so the traditional long-range hypernetted chain (HNC) resummation does not apply to the present situation. It is therefore replaced by the much more rapidly decaying chains made of three-bubbles or other compact nonconvolution graphs. The number of graphs within each order is also drastically reduced.

A.  $\nu \leq 2$  nodal expansion

Let us first pay attention to the lower dimension where the rule(c) is simpler. The three distinct first-order corrections to the potential of average force are given as ( $i, j$  being the electron or ion)

$$C_{ij}^{(1)}(r) = -\frac{Z_i Z_j \Lambda_e}{2^{\epsilon/2} \Gamma(1 + \frac{\epsilon}{2})} \cdot \frac{K_{\epsilon/2}(r/\lambda_D)}{(r/\lambda_D)^{\epsilon/2}}, \quad Z_{i,j} = \pm 1 \tag{3.6}$$

an obvious extension of the OCP result.  $K_\nu(x)$  is the second kind modified Bessel function.

High-order corrections start with  $l - k = 2$ .  $l$  and  $k$  denote, respectively, the number of lines and field points within a given nodal graph. As shown on Fig. 1, rule (d) reduces drastically the number of available diagrams, as compared to the OCP's. In the present situation, we therefore obtain

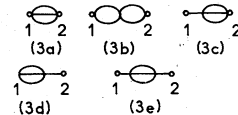
$$C_{ij}^{(2)}(r) = \frac{[C_{ij}^{(1)}(r)]^2}{2!}, \quad C_{ij}^{(3a)}(r) = \frac{[C_{ij}^{(1)}(r)]^3}{3!}. \tag{3.7}$$

The second (3b) is the convolution product of two bubbles ( $Z_i^2 = Z_j^2 = 1$ )

1. Second order



2. Third order



3. Fourth order

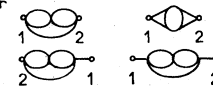


FIG. 1. Two-component plasma nodal graphs. The solid line denotes the Debye line [Eq. (3.11')].

$$G_{ij}^{(3b)}(r) = \frac{K_{\nu-1} S_{\nu-1}^2 \Gamma(\frac{1}{2}(\epsilon+1))^2 \Gamma(1-\frac{1}{2}\epsilon)^2}{2^{5+3\epsilon/2} \Gamma(1+\frac{1}{2}\epsilon)^3 \pi^{3/2} r^{\epsilon/2}} \Lambda_\epsilon^3 \int_0^\infty dk k^{1+\epsilon/2} J_{\epsilon/2}(kr) {}_2F_1(1, 1-\frac{1}{2}\epsilon; \frac{3}{2}; -\frac{1}{4}k^2)^2, \quad (3.8)$$

where  $K_\nu = S_\nu (2\pi)^{-\nu}$ . Equation (3.8) is suitable for numerical computation with  $r$  in number of  $\lambda_D$ , as a running parameter. The graphs (3c, 3d) may be worked out similarly through

$$G_{ij}^{(3c, 3d)} = \frac{Z_i Z_j}{3!} \frac{K_{\nu-1}^2}{(2\pi)^{2\nu}} \frac{\Lambda_\epsilon^3}{2^{\epsilon/2}} S_{\nu-1} \frac{\sqrt{\pi} \Gamma(\frac{1}{2}(\epsilon+1))}{\Gamma(1+\frac{1}{2}\epsilon)^4 r^{\epsilon/2}} \int_0^\infty \frac{dk k J_{\epsilon/2}(kr)}{k^2+1} \int_0^\infty du u^{1-\epsilon} K_{\epsilon/2}^3(u) J_{\epsilon/2}(ku). \quad (3.9)$$

(3e) is obtained by adding one more  $(k^2+1)^{-1}$  under the  $k$  quadrature.

The present analysis works only for  $\epsilon > -1$ . It cannot be straightforwardly extended to high orders, in view of  $K_{\epsilon/2}^P(u) \sim u^{-P|\epsilon|/2}$  when  $u \rightarrow 0$ . Short-range resummations of  $n$ -bubbles lines should then be used to all order in  $\Lambda_\epsilon$ , in order to get rid of this difficulty. The present order by order evaluation of the nodal graphs is expected to remain valid in the  $\epsilon = 0$  limit, on both sides of the cross over dimension  $\nu = 2$ . By extrapolating the above third-order results, one gets the domi-

nant asymptotic contribution within each order from the alternate chains built up from three bubbles intertwined with single Debye lines. Therefore, a modified version of the standard OCP Hypernetted chain approximation with three bubbles replacing two bubbles, and lacunary series instead of the geometric ones is expected to exhaust  $g_2(r)$  in the  $r \rightarrow \infty$  limit. On the other hand, the short-range limit  $\lim_{r \rightarrow 0} g_2(r)$  is no longer monitored by the resummations of ladder graphs when  $\nu < 2$ .

The long-range resummation explained by

$$W_2^{ij}(r) \simeq \left(\frac{2}{r}\right)^{\epsilon/2} \Lambda_\epsilon^2 Z_i Z_j \int_0^\infty dk k^{1+\epsilon/2} J_{\epsilon/2}(kr) \left( \frac{\Lambda_\epsilon k^2}{(k^2+1)} \frac{G_3(k)}{[1+1/k^2 - \Lambda_\epsilon G_3^{1/2}(k)]} - \frac{G_3(k)}{(1+1/k^2)^2 - \Lambda_\epsilon^2 G_3(k)} - G_3(k) \right) \quad (3.10)$$

when

$$\left| \Lambda_\epsilon k^2 G_3^{1/2}(k) / (k^2+1) \right| \leq 1,$$

produces the required extension of the HNC schema. The sign “ $\simeq$ ” accounts for the obvious but cumbersome  $\nu$ -dependent overall factor.

#### B. $\nu > 2$ nodal expansion

Most part of the above discussion is expected to hold for  $\nu > 2$ , provided due attention is paid to rule (c), with a first-order Debye interaction in the  $\nu = 3$  form. Therefore, only a slight algebraic modification of the  $\nu < 2$  treatment is needed. However, this latter is sufficient to produce more complications. This is why we detailed first the basic features of the TCP nodal expansion using the more symmetrical and transparent  $\nu < 2$  situation. Following rule (c), the normalized first-order Debye line in  $k$  space is now given as

$$H'(k) = -\frac{S_{\nu-1} \sqrt{\pi} \Gamma(\frac{1}{2}(\epsilon+1))}{4\Gamma(1+\frac{1}{2}\epsilon)} \times \left( \frac{1}{k^2+1} + \frac{2(\alpha_2^2 - \alpha_1^2)}{(k^2 + \alpha_1^2)(k^2 + \alpha_2^2)} + \frac{\alpha_2'^2 - \alpha_1'^2}{(k^2 + \alpha_1'^2)(k^2 + \alpha_2'^2)} \right) \quad (3.11)$$

extrapolating first the real case  $\nu = 3$ , where the pair  $(\alpha_1, \alpha_2)$  refers to the plus-minus pair, while

$(\alpha_1', \alpha_2')$  pertains to the diffraction corrections<sup>11,12</sup> of the lighter particles (“electrons”). For the sake of simplicity, we shall ignore these latter in what follows. Taking the classical limit  $\alpha_2 \rightarrow \infty$ ,  $\alpha_1 - 1$  produces

$$H'(k) = -\frac{S_{\nu-1} \sqrt{\pi} \Gamma(\frac{1}{2}(\epsilon+1))}{2\Gamma(1+\frac{1}{2}\epsilon)} \times \left( \frac{1}{k^2+1} + \frac{\alpha_2^2 - \alpha_1^2}{(k^2 + \alpha_1^2)(k^2 + \alpha_2^2)} \right) \quad (3.11')$$

in  $k$  space and

$$C_{ij}^{(1)}(r) = -\frac{Z_i Z_j \Lambda_\epsilon}{2^{1+\epsilon/2} \Gamma(1+\frac{1}{2}\epsilon) r^{\epsilon/2}} \times [K_{\epsilon/2}(r) + \alpha_1^{\epsilon/2} K_{\epsilon/2}(\alpha_1 r) - \alpha_2^{\epsilon/2} K_{\epsilon/2}(\alpha_2 r)] \quad (3.12)$$

in  $r$  space, with  $r$  and  $\alpha_{1,2}$  in number of  $\lambda_D$  and  $\lambda_D^{-1}$ , respectively. In the  $T \rightarrow \infty$  limit, the latter reduces to the  $\nu \leq 2$  result (3.6). As far as their derivation is concerned, these expressions make sense only for  $\nu = 3$ . Nevertheless, we find it useful to explain them as  $\epsilon$ -dependent expressions, continuing analytically the integer Debye quantities to  $\epsilon > 0$ . Such a procedure allows for an intrinsic rephrasing of the TCP nodal expansion when bound states are likely to appear. Again, high-order nodal graphs may be estimated as above, from Eqs. (3.11) and (3.11') and the corresponding two-bubble function  $G_2(k)$ .

IV. FINAL CALCULATION OF  $D_{\perp}$

Up to now, the TCP nodal equilibrium properties are detailed enough to allow the completion of the calculation of the transverse velocity coefficient  $D_{\perp}$  as given by Eq. (2.22). The only remaining task is to explain the  $S_{ij}(k)$ 's introduced in Eq. (2.12) through the linearized pair correlation function

$$g_2^{ij}(r) \sim 1 + W_2^{ij}(r), \quad \Lambda_e \ll 1. \quad (4.1)$$

It is important to note that the sum  $\mathcal{C}(k)$  is essentially built upon the more compact nodal graphs which decay faster than first order (Debye). They are depicted in Fig. 2.

Their convolutions with one and two Debye lines are to be included too, so that the general quantity to be inserted in Eq. (2.15) is

$$\begin{aligned} \mathcal{C}(k) &\equiv -S_{ee}(k) - S_{ii}(k) + 2S_{ei}(k) \\ &\simeq -W_2^{ii}(k) - W_2^{ee}(k) + 2W_2^{ei}(k) \\ &= 4 \left( H'(k) + \sum_{n=3}^{\infty} B(k) [1 + H'(k)]^n \right) \\ &\equiv 4H'(k) + \mathcal{C}'(k), \end{aligned} \quad (4.2)$$

where  $B(k)$  denotes the (bubble) sum, within a given order  $n$ , of the above listed graphs. The first remarkable result is the absence of second-order contribution. The more important diagrams in the  $k \rightarrow 0$  limit are the linear chains built upon three bubbles intertwined with Debye lines. The first one appears with  $n=5$ .  $H'(k)$  and  $B(k)$  are obtained from the nodal analysis performed in Sec. III. However, the most important property discussed in the present work is the negligible contribution left by all the higher-order graphs to the expression (2.22) when the integration procedure (2.23) is applied to it, so that

$$\int_{2\pi/L}^{k_D^{-1}} dk_{\perp} \mathcal{C}'(k) k_{\perp} \simeq 0. \quad (4.3)$$

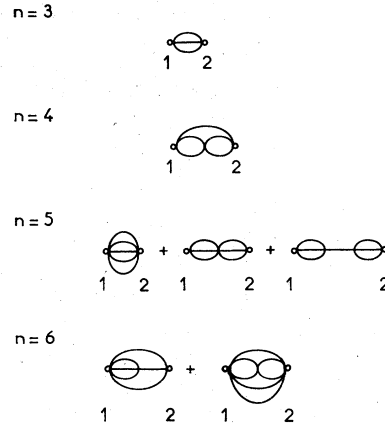


FIG. 2. Two-component plasma nodal graphs contributing to  $D_{\perp}$ .

This is a result of the fast decaying properties of the integrand in the  $k \rightarrow 0$  limit, conveying much of the particle transport across the magnetic field. As a consequence, the usual first-order derivation of the Bohm transverse diffusion appears very efficient treatment which almost completely eliminates any contribution from the higher orders in  $\Lambda_e$ . Moreover it can be worked out continuously for any dimensionality  $2 \leq \nu \leq 3$ . Therefore, the expression (2.22) for  $D_{\perp}$  explained by its first order<sup>1,2</sup>

$$\begin{aligned} D_{\perp} &= \sqrt{2} \frac{ck_B T}{eB} \Lambda_0^{1/2} \left[ \ln \left( \frac{R}{2\pi\lambda_D} \right) \right]^{1/2}, \quad \nu=2 \\ &= \frac{ck_B T}{eB} \left( \frac{\Lambda_1}{2} \right)^{1/2} \left( \frac{\lambda_D}{R} \ln \frac{R}{2\pi\lambda_D} \right)^{1/2}, \quad \nu=3 \end{aligned} \quad (4.4)$$

integer quantities appears as remarkably stable with respect to the high-order  $\Lambda_e$  corrections.

<sup>1</sup>J. B. Taylor and B. McNamara, *Phys. Fluids* **14**, 1492 (1971).

<sup>2</sup>D. Montgomery, *Les Houches Lectures Notes* (Gordon and Breach, New York, 1975); also D. Montgomery and F. Tappert, *Phys. Fluids* **15**, 683 (1972); D. Montgomery, C. S. Liu, and G. Vahala, *ibid.* **15**, 815 (1972); G. Vahala, *Phys. Rev. Lett.* **29**, 93 (1972); *Phys. Fluids* **16**, 1876 (1973).

<sup>3</sup>J. A. Krommes and C. Oberman, *J. Plasma Phys.* **16**, 229 (1976); see also, S. Ichimaru and M. N. Rosenbluth, *Plasma Physics and Controlled Nuclear Fusion* (IAEA, Vienna, 1971), Vol. II, p. 373.

<sup>4</sup>C. Deutsch, (unpublished).

<sup>5</sup>R. N. Parker, *Bull. Am. Phys. Soc.* **20**, 1372 (1975).

<sup>6</sup>K. A. Brueckner and S. Jorna, *Rev. Mod. Phys.* **46**,

325 (1974).

<sup>7</sup>C. Deutsch, *J. Math. Phys.* **17**, 1404 (1976); and **18**, 1297 (1977).

<sup>8</sup>K. G. Wilson, *Phys. Rev. Lett.* **28**, 548 (1972); and *Phys. Rev. D* **7**, 2911 (1973).

<sup>9</sup>B. Mandelbrot, *Les Objets Fractals* (Flammarion, Paris, 1975).

<sup>10</sup>Actually, this could be achieved by prescribing a suitable measure on the fractal ensemble. This point will be considered in a forthcoming work. However, we can explain the geometric content of the variable dimensionality as follows: The combined effect of the other particles and  $\vec{B}$  results in a complicated motion spanning less than the usual three-dimensional available space, in analogy with similar processes



in neutral fluid turbulence. The three-dimensional particle trajectory shows then a kind of Peano-like behavior, i.e., it can reach any point of the plasma container within an arbitrary small prescribed distance.

<sup>11</sup>C. Deutsch and M. M. Gombert, J. Math. Phys. 17, 1017 (1976).

<sup>12</sup>They are important for  $k_B T \geq 1$  Ry in  $\nu=3$ .

<sup>13</sup>I.e.,  $T > 157\,000^\circ\text{K}$ .